し、抗炎症作用を持つ。また、in vitro で活性酸素による軟骨細胞傷害を抑制し、ヒアルロン酸の分解にも抑制作用を示した。OA に対する TS-234(100mg/回)の関節腔内投与の他施設二重盲検群間比較試験が行われたが、有用性を示すには至っていない[2]。最近の報告では、細胞外 SOD (EC-SOD) 遺伝子を感染導入した EC-SOD 過剰発現細胞の皮下投与により、コラーゲン誘導関節炎が有意に抑制されている[3]。他方、O_2^- 存在下で NO が産生された場合には、NO によって O_2^- が消化されることにより細胞障害が抑制されるが、反応生成物である peroxynitrite ($ONOO^-$) は強い酸化活性を持ち、ミトコンドリアのクエン酸回路中のアコニターゼを不活化したり、脂質の過酸化によって組織細胞障害性に働くといわれる。

2.4 関節炎と NO

関節炎において IL-1, TNF-α といったサイトカインは MMP (matrix metalloproteinase) の誘導を通じてマトリックス破壊に関与したり、プロテオグリカン産生を抑制するほか、iNOS や COX (cyclooxygenase)-2 などの炎症のメディエーターを誘導して、滑膜炎と軟骨破壊に中心的な役割を果たす。破壊される側の軟骨細胞も炎症性サイトカン刺激により iNOS を発現し、プロテオグリカン産生は抑制される。軟骨組織の器官培養では、OA 軟骨は無刺激で NO や PGE_2 を産生する。培養軟骨細胞では、IL-1, TNF-α , IL-17, IL-18 といった炎症性サイトカインや LPS (lipopolysaccharide)刺激による iNOS の発現誘導がみられる[4]。iNOS が一旦発現すると、他のアイソフォームの 1,000 倍以上の持続的・高濃度の NO が産生されることがわかっており、生体防御的に働くか、組織傷害性に働くかはその局所濃度に依存するといわれる。軟骨組織中では表層の軟骨細胞が深層に比して IL-1 刺激に対する反応性が高い[5]。実際に関節リウマチ (RA) や OA 患者の関節液や組織中では正常に比して高いレベルの NO が検出される[6]。

関節炎における NO 産生機構

NO は反応性の高いラジカルであり、NO 合成酵素(NOS)の働きにより L-アルギニンから生成され、同時に L-シトルリンを生じる。NO 合成を触媒する NOS のうち、neuronal constitutive NOS (ncNOS), endothelial constitutive NOS (ecNOS) は構成的 NOS (cNOS) と呼ばれ、細胞内カルシウムイオン濃度 $[Ca^{2+}]$ i によりカルモジュリン依存性に活性化され、心血管系や中枢神経系といった生体の恒常性維持にかかわる。一

方、iNOS は IL-1, 17, 18, TNF-α などのサイトカインや LPS によって炎症時に誘導され、$[Ca^{2+}]$ i 非依存性に活性化される。これら誘導刺激は MAPK (mitogen-activated protein kinase) を中心としたシグナル伝達機構によって核に伝達され、NF-κB の転写活性化を通して iNOS 遺伝子の発現が誘導される。NF-κB は p50 (NF-κB1) と p65 (RelA) のヘテロ二量体で、通常 I-κB と複合体を形成して不活性型として細胞質に局在している。Iκ-B はサイトカイン、LPS などの刺激後にリン酸化、ユビキチン化を受け、プロテアソームによる分解を受ける。Iκ-B の解離により NF-κB は活性化され、速やかに核内に移行してターゲットとなる DNA のκB 配列 (GGGGACTTTCC) に結合し、NOS、COX-2 の他、種々の炎症性サイトカインや接着分子の転写活性化、蛋白産生を促す。MAPK スーパーファミリーの p38 のインヒビターである SB202190 や、NK-κB のインヒビターである PDTC (pyrrolidine dithiocarbamate) はヒト OA 軟骨細胞において IL-17 による iNOS 発現、NO 産生を抑制する[7]。Mendes ら[8] はウシ軟骨細胞を IL-1 (5 ng/ml) で NO 放出剤である SNAP の存在、非存在下に刺激、EMSA にて NF-κB および AP-1 の活性化を、Northern blot で iNOS mRNA の発現レベルを、Western blot で I-κB, nNOS, iNOS の蛋白レベルでの発現を検討した。SNAP は IL-1 により誘導される NF-κB 活性化と iNOS 発現を抑制し、IL-1 とほぼ同等に AP-1 を活性化したことから、NO は IL-1 による NF-κB、あるいは AP-1 の活性化を制御すると考えられた。

2.5 NO による軟骨破壊 (図 4.2.1)
2.5.1 軟骨細胞のアポトーシス

OA の病態において軟骨細胞のアポトーシスは重要とされ、軟骨組織中の唯一の基質産生細胞である軟骨細胞の減少により軟骨修復が妨げられたり、軟骨変性が進展すると考えられる。NO や Fas がその原因として報告されているが、その他の誘因、例えば低酸素、基質のアシドーシス、異常なメカニカルストレス、向炎症性サイトカインの影響については検討が始まったばかりである。また、IGF-1 などの成長因子や抗炎症性のサイトカインがアポトーシスを抑制できるかについてもほとんど検討されていない。

2.5.2 NO と軟骨細胞のアポトーシス

培養軟骨細胞に NO ドナーである SNP (sodium nitroprusside) を作用させると、軟骨細胞のアポトーシスが誘導される。一方、IL-1 を作用させると NO 産生は強く誘導されるが、アポトーシスは生じない[9]。こ

のことは、内因性の NO のみではアポトーシスが誘導されないことを示している。他方、in vivo では、関節炎の軟骨組織において正常（～5%）に比べて明らかに多くのアポトーシスに陥った軟骨細胞が認められる。電子顕微鏡による観察でも、細胞の縮小、核の濃縮像を伴うアポトーシスが観察される一方、死細胞の断片やアポトーシス小体もマトリックス内に認められる[10]。さらに過剰に産生された NO は、NO そのものによる直接的細胞障害に加えて、peroxynitrite（ONOOH）などの NO 由来の反応性窒素酸化物の生成を経て、多彩な病態生理活性を発揮する。ONOOH は強力な酸化剤で、SH 基の酸化や脂質の過酸化などを引き起こして細胞に傷害を与えるとともに、DNA とも反応し傷害を与え、細胞傷害やアポトーシスをもたらすことが知られている。Loeser らは酸化ストレスの指標にニトロチロシンの染色性を用いて、若年および老齢サル、ヒト OA の軟骨組織を検討した[11]。ニトロチロシン染色性は年令および OA 変化に関連しており、また同時に行った IL-1β の染色性と一致した。一部の老齢サル軟骨では IL-1 の存在なしに NT 染色性が亢進しているものがあり、年齢に関連した酸化ストレスは IL-1 非依存性であることが示唆された。OA 軟骨

組織の免疫組織染色では、TUNEL 陽性細胞、ニトロチロシン陽性細胞（NO による組織内チロシン残基ニトロ化の指標）と Caspase-9 および Caspase-3 発現細胞の分布はよく一致する。また、組織学的 OA グレード、ニトロチロシン陽性率、TUNEL 陽性率は活性化 Caspase-3 陽性率と強く相関するが、RA 軟骨組織においては、NO によるアポトーシス以外の細胞死が生じている可能性があり、さらに検討が必要である[12,13]。一方で Greisberg ら[14] は NT 陽性細胞と TUNEL 陽性細胞は必ずしも一致しないことを二重染色で確認し、NO は軟骨細胞アポトーシスの直接的な一次シグナルとは考えにくいと結論している。

2.5.3 メカニカルストレスと NO

正常関節では、関節運動に伴う応力負荷を筋肉、腱、靱帯によって適切に吸収、分散し、関節に直接の衝撃がかからないように巧妙な神経支配を受けている。OA ではこの応力分散機構が破綻しており、異常な力学的負荷により関節軟骨は種々の程度に変性し、次第にその特有の粘弾性を失っていく。軟骨の変性に伴い、関節軟骨にかかる強い衝撃は軟骨下骨にほぼ直接伝播されることになり、軟骨下骨の微小骨折、それに引き続くリモデリングが生じる。これは X 線上骨硬化
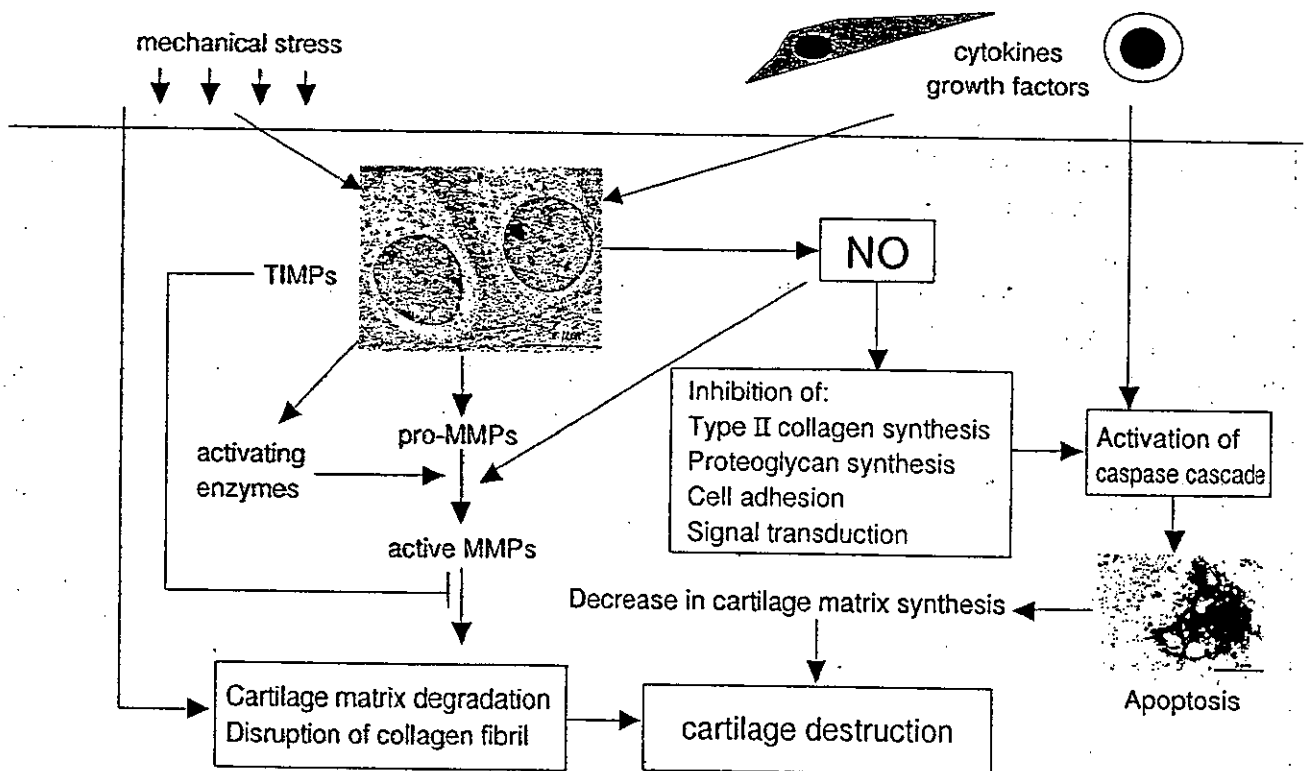

図 4.2.1 OA 軟骨破壊における NO の関与

像として認められるが、軟骨下骨もまた正常なショック吸収体としてはもはや有効には働かない。軟骨細胞に対するメカニカルストレスを *in vitro* で再現する方法としてはこれまで、静的圧負荷、伸張ストレス、shear ストレスなどさまざまな方法が試みられている。また、ストレスの条件を変えたり、ストレスの種類や細胞培養の条件によって、軟骨細胞は異なる反応を示すことも知られている。

Lee ら[15]によると、OA 軟骨細胞では shear ストレスに応じて負荷および時間依存性に NO 産生が亢進する。静水圧はこの NO 産生を抑制するが、ストレスなしでも内因性 NO には影響を与えない。Shear stress あるいは NO 供与体により産生された NO はアグリカン、II 型コラーゲンの mRNA レベルを下げた。間欠的圧負荷は SNP によるこの抑制効果をブロックしたが、shear stress による遺伝子発現に影響を与えなかった。おそらく生体内でも異なる負荷のバランスにより、軟骨基質の代謝が制御されていると考えられる。一方、Islam ら[16]は持続的な静水圧は 5 Mpa、4 時間、1 Hz で DNA fragmentation、Caspase-3 活性化、PARP の分解による軟骨細胞のアポトーシスを誘導することを報告している。RT-PCR および Western blotting による検討の結果、4 時間で p53, c-myc, bax-α の発現亢進、2 時間で bcl-2 の発現低下を伴った。Real-time RT-PCR では 2 時間で TNF-α、4 時間で iNOS の mRNA レベルでの発現亢進を認めた。

また、これまでの実験的 OA モデルの多くは、靱帯切離により *in vivo* で異常なメカニカルストレスを誘導するものが多く、また薬効評価にも用いられる。Hashimoto ら[17]は前十字靱帯切離による実験的 OA モデルにおいて、無処置対照膝軟骨の 6.3% に軟骨細胞のアポトーシスがみられるのに対し、ACLT 膝軟骨では 28.7% の軟骨細胞にアポトーシスがみられること、TUNEL 陽性細胞率と OA グレードあるいは NO 産生量が相関することを報告している。

2.5.4 NO を介する軟骨組織破壊と軟骨細胞のアポトーシス

最近では、軟骨周囲のマトリックスの変性あるいは減少が caspase の活性化を促し、軟骨細胞にアポトーシスを誘導する可能性が示唆されている[18]。NO の軟骨細胞および基質に与える影響としては、①II 型コラーゲン、プロテオグリカン産生抑制、②MMPs の活性化、③β₁ インテグリンを介した細胞内シグナル伝達の阻害などが明らかとなっている[18]。ことに軟骨マトリックス破壊に重要な役割を果たす MMPs の活性化

は各種コラーゲン、プロテオグリカンやフィブロネクチン、ラミニンといった糖蛋白を分解することで軟骨細胞の基質への接着を障害して軟骨細胞のアポトーシスを誘導する可能性もある。

2.6 アポトーシスのシグナル伝達経路

アポトーシスのシグナル伝達経路には、①ミトコンドリア経路、②直接の DNA 障害、p53 を介する経路、③セラミドによる経路、④ Fas-Fas ligand などの death domain を介する経路、⑤カルシウム－カルモデュリン経路などがあり、それぞれ特有のカスペースファミリーを活性化して細胞をアポトーシスへと導く。最終的に核クロマチンの濃縮、DNA の断片化はそれぞれ活性化 caspase-3 の核ラミンの切断、DNase の活性化により生じ、caspase-3 はさらに細胞内アクチンフィラメントの分解により細胞膜の budding によるアポトーシス小体の形成に働く。NO あるいは ONOOH はミトコンドリアに作用して PARS (poly ADP-ribose synthase) の活性化により、エネルギー代謝を損なう可能性があるが、一方で OA 軟骨組織においては、正常軟骨に比してアポトーシス促進蛋白である Bax 発現率に差を認めず、アポトーシス抑制蛋白である Bcl-2 の発現が減少していることも報告されている[19]。Bax はミトコンドリアの膜上にある複合蛋白 PT pore の VDAC (voltage-dependent anion channel) に直接作用してミトコンドリアの脱機能をもたらし、Bcl-2 は VDAC に結合して PT pore を閉口させるモデルも提唱されている。我々は OA の早期には軟骨細胞のミトコンドリアにおける Bcl-2, Bax の不均衡が生じ、cytochtome c の遊離、caspase-9 の活性化、続いて caspase-3 の活性化が生じて最終的に軟骨細胞にアポトーシスをもたらすのではないかと考えている。

Kim ら[20]によると NO 処理は p38 MAPK を介した経路により p53 蛋白レベルでの増加、caspase-3 活性化を経て軟骨細胞にアポトーシスを誘導する。NO により誘導された p38 kinase 活性化は NF-κB 活性化を引き起こし、一方で p53 遺伝子の転写を促す。野生型 p53 発現は NO 誘導の軟骨細胞アポトーシスを亢進させるが、dominant negative p53 はこれをブロックすることから、p53 が NO 誘導アポトーシスに重要な役割を持つと考えられる。p53 蛋白の集積は Bax 発現亢進を経てミトコンドリアからの cytochrome c の遊離、caspase の発現を引き起こす。NO により活性化された p38 kinase は NF-κB による転写活性化と直接の p53 リン酸化という 2 つの経路により、軟骨細胞にア

ポトーシスを誘導すると考えられる。

2.7 NO 制御による軟骨破壊の抑制
2.7.1 NO 産生阻害による制御

　NO は生体防御的にも、傷害性にも働きうる両刃の剣であるが[21]、OA や RA の軟骨破壊に対しても NOS の阻害による NO 産生抑制の効果が報告されている。ウサギの培養軟骨細胞において NOS 阻害剤である NG-monomethyl-L-arginine（L-NMA）は、IL-1 誘導による NO 産生亢進およびプロテオグリカン産生抑制を阻害する[22]。イヌの ACL 切離 OA モデルでは iNOS の選択的阻害剤である N-iminoethyl-L-lysine（L-NIL）の投与により、軟骨変性、骨棘形成が有意に抑制され、組織学的な検討でも L-NIL 投与群において iNOS, nitro-tyrosine, COX-2, MMP-1, 3 の発現率が減少する[23]。さらに同様の系において軟骨細胞のアポトーシスと caspase-3 の発現率も NOS 阻害剤により低下することも報告されている[24]。

　Mathy-Hartert ら[25] は NOS 阻害剤（L-NMMA）、抗酸化剤（NAC）、NSAID（Aceclofenac）がヒト OA 軟骨細胞の IL-1, NO, PGE_2 産生に与える影響を調べた。LPS（10 μg/ml）は IL-1β , iNOS, COX-2 の発現を強く誘導し、培養液中でも NO および PGE_2 量も増加した。一方、0.5 mM の L-NMMA 処理は NO 産生を強く抑制する一方で、転写レベルの変化を介さずに PGE_2 産生を増加させた。逆に NAC 処理は IL-1β および iNOS mRNA 発現亢進とともに NO 産生を亢進させたが、COX-2 mRNA には有為な影響を与えず、COX-2 蛋白および PGE_2 産生は変化がなかった。Aceclofenac は COX-2 mRNA 発現に影響を与えることなく、PGE_2 産生を抑制した。以上から、ROS は LPS による軟骨細胞の IL-1β , NO, PGE_2 産生を個々にコントロールしており、抗酸化剤による治療はターゲットとする ROS によって異なる効果を持つことが示唆される。

　また、SCW（streptococcal cell wall fragments）誘導関節炎は関節炎発症後でも NOS 阻害剤 NMMA（NG-monomethyl-L-arginine）によって抑制されること[26]、iNOS 選択的阻害剤がアジュバント関節炎を抑制すること[27] が報告されている。一方、我々は iNOS ノックアウトマウスにコラーゲン関節炎を誘導して、軟骨破壊の評価を行った[28]。NOS2-/- マウスはコラーゲン関節炎抵抗性であるが、Terato らの抗 II 型コラーゲン抗体カクテルを用いた autoantibody mediated arthritis は惹起できる。関節炎の程度は野生型に比べるとやや軽度であり、関節炎誘導後 14 日での膝関節軟骨の組織スコアも有意に低値を示した。TUNEL 陽性細胞、ニトロチロシン陽性細胞率も有意に低値であったが、血中 IL-1 値には差がなく、軟骨組織中の MMP-3, MMP-9 の陽性率にも差を認めなかった。このことから、NOS2 を欠失したマウスにおいても IL-1 の産生亢進および MMP の活性化による関節軟骨破壊は抑制しきれず、RA 軟骨破壊に対する NOS 阻害剤の効果にも限界があることが示唆される。

2.7.2 シグナル伝達阻害による NO 生成阻害

　Badger らによると、p38 MAPK の阻害剤 SB242235 はウシ軟骨細胞のプロテオグリカン（PG）産生に影響を与えず、また IL-1α による PG 喪失にも影響を持たないが、IL-1α により誘導される iNOS mRNA 発現、NO 産生は用量依存性に抑制する[29]。ところが、ヒト軟骨細胞では IL-1β による p38 MAPK 誘導は SB242235 により抑制されたが、iNOS 発現、NO 産生は抑制されない。p38 阻害剤による iNOS 発現のコントロールには種によって違いがあることを示しており、興味深い。

2.7.3 抗サイトカイン療法

　Goodstone ら[30] は、ブタ軟骨細胞では TNF-α は IL-1 より強力に（約 50 倍）NO 産生を誘導すること、ほぼ同等のアグリカン合成抑制能を持つこと、その抑制効果は iNOS 阻害剤により緩和されることを報告した。また、ともにヒアルロン酸合成を刺激したが、iNOS 阻害剤による影響はなかった。

　Relic ら[31] によると、ヒト培養軟骨細胞あるいは軟骨片をまず TNF-α で 24 時間処理後、さらに SNP により 24 時間処理すると、SNP による DNA fragmentation や Annexin V 結合性でみるアポトーシスが著明に抑制された。TNF-α は NF-κB の活性化を誘導しており、アポトーシス抑制効果は NF-κB の inhibitor で消失した。また TNF-α は COX-2 発現を誘導し、COX-2 の阻害剤は TNF-α の抗アポトーシス効果に拮抗した。以上により、TNF-α は NF-κB の活性化を通じて NO 誘導軟骨細胞アポトーシスを抑制し、これには COX-2 の活性化を必要とすることが示唆される。

　一方、Vuolteenaho ら[32] はヒト OA 軟骨片を用いて、TNF-α アンタゴニストである infliximab（抗 TNF-α 抗体）と etanercept（可溶性レセプター抗体）の NO 産生に対する影響を調べた。infliximab と etanercept はともに TNF-α による NO 産生を用量依存性に抑制したが、IL-1, IL-17, LPS による NO 産生は抑制できなかった。OA 軟骨は TNF-α および可溶性の TNF-α 受容体（TNFRI と TNFRII）を内因性に産生しており、可溶性 TNFRI に対する中和抗体は無刺激での NO 産生を増加

させたが、可溶性 TNFRII に対する中和抗体では変化がなかった。従って OA 軟骨では内因性に産生される可溶性の TNFRI が TNF-α による NO 産生をコントロールしていると考えられる。

2.7.4 サイトカインによる NO 産生抑制

IL-4, IL-10, IL-13 といった抗炎症性サイトカインは IL-1 や TNF-α といった炎症性サイトカインに拮抗する。Wang ら[33] の報告によると、ラット軟骨細胞において IL-10 (20 ng/ml) は IL-1 に拮抗して細胞死を抑制し、iNOS および MMP-3 の発現を抑制した。(Wang Y, 2001) 我々の最近の研究では、IL-4 は伸張ストレスにより発現が亢進する iNOS mRNA レベルを用量依存性に低下させる。また、IL-4 と IL-10 の同時投与は軟骨細胞による IL-1ra (receptor antagonist) の産生量を変えることなく IL-1 および TNF-α の発現を抑え、結局 IL-1/IL-1ra 比を減少させることにより、軟骨保護的に作用する[34]。

2.7.5 転写因子を介した NO 産生制御

PPAR (peroxisome proliferaion-activated receptor) γ は細胞内の蛋白発現を調節する核内受容体の一つで、レチノイド X 受容体 (RXR) とヘテロ二量体を形成して DNA のエンハンサー、サイレンサー領域に結合し、iNOS、COX-2 をはじめ、種々の蛋白の発現をコントロールしている。サブタイプの一つである PPAR γ の活性化は NF-κB と共通の co-activator (CBP/p300, SRC-1) をめぐって拮抗するため、NF-κB の転写活性、ひいては炎症を抑制する。最近、チアゾリン系薬剤 (TZD) および内因性リガンドである 15d-PGJ$_2$ が、コラーゲン関節炎を抑制することが報告された[35]。興味深いことに、軟骨細胞も PPARα, PPARγ を発現しており[36]、PPARγ リガンドは IL-1 による軟骨細胞のプロテオグリカン産生抑制ならびに NO 産生作用にも拮抗する。今後、こういった転写活性の制御による軟骨破壊の抑制も試みられるようになると思われる。

文献

1) Mendes AF, Caramona MM, Carvalho AP, Lopes MC: Differential roles of hydrogen peroxide and superoxide in mediating IL-1-induced NF-kappaB activation and iNOS expression in bovine articular chondrocytes. J Cell Biochem 88(4): 783-93, 2003

2) 小松原良雄、浅井富明、中野重行ほか：変形性関節症に対する TSA-234 (rhSOD) の至適用量設定試験。リウマチ 35: 621-35, 1995

3) Iyama S, Okamoto T, Sato T et al: Treatment of murine collagen-induced arthritis by ex vivo extra-cellular superoxide dismutase gene transfer. Arthritis Rheum 44: 2160-7, 2001

4) 金田博志、本田　恵、鎌田俊之：superoxide dismutase (SOD) 活性について。整形外科 MOOK 32: 168-174, 1984

5) Fukuda K, Kumano F, Takayama M et al: Zonal differencies in nitric oxide synthasis by bovine chondrocytes exposed to interleukin-1. Inflamm Res 44: 434-7, 1995

6) Farrell AJ, Blake DR, Palmer RM et al: Increased concentration s of nitrite in synovial fluid and serum samples suggest increased nitiric oxide synthesis in rheumatic diseases. Ann Rheum Dis 51: 1219-22, 1992

7) Martel-Pelletier J, Mineau F, Jovanovic D et al: Mitogen-activated protein kinase and nuclear factor kappaB together regulate interleukin-17-induced nitric oxide production in human osteoarthritic chondrocytes:possible role of transactivating factor mitogen-activated protein kinase-activated protein kinase-activated protein kinase (MAPKAOK). Arthritis Rheum 42: 2399-409, 1999

8) Mendes AF, Carvalho AP, Caramona MM et al: Role of nitric oxide in the activation of NF-kappaB, AP-1 and NOS II expression in articular chondrocytes. Inflamm Res 51(7): 369-75, 2002

9) Blanco FJ, Ochs RL, Schwarz H et al: Chondrocyte apoptosis induced by nitric oxide. Am J Pathol 146: 75-85, 1995

10) 西田圭一郎、松尾真嗣、加藤久佳ほか：関節軟骨破壊と NO。現代医療 Vol.33, No.5: 57-62, 2001

11) Loeser RF, Carlson CS, Del Carlo M et al: Detection of nitrotyrosine in aging and osteoarthritic cartilage: Correlation of oxidative damage with the presence of interleukin-1beta and with chondrocyte resistance to insulin-like growth factor 1. Arthritis Rheum 46(9):2349-57,2002

12) Matsuo M, Nishida K, Yoshida A et al: Expression of caspase-3 and -9 relevant to cartilage destruction and chondrocyte apoptosis in human osteoarthritic cartilage. Acta Med Okayama 55: 333-40, 2001

13) 西田圭一郎、井上　一、松尾真嗣ほか：軟骨破壊における一酸化窒素の役割。最新医学 別冊、リウマチ 2000: 88-99, 2000

14) Greisberg J, Bliss M, Terek R: The prevalence of nitric oxide in apoptotic chondrocytes of osteoarthritis. Osteoarthritis Cartilage 10(3): 207-11, 2002

15) Lee MS, Trindade MC, Ikenoue T et al: Intermittent hydrostatic pressure inhibits shear stress-induced nitric oxide release in human osteoarthritic

chondrocytes *in vitro*. J Rheumatol 30(2): 326-8, 2003

16) Islam N, Haqqi TM, Jepsen KJ et al: Hydrostatic pressure induces apoptosis in human chondrocytes from osteoarthritic cartilage through upregulation of tumor necrosis factor-alpha, inducible nitric oxide synthase, p53, c-myc, and bax-alpha, and suppression of bcl-2. J Cell Biochem 87(3): 266-78, 2002

17) Hashimoto S, Takahashi K, Amiel D et al: Chondrocyte apoptosis and nitric oxide production during experimentally induced osteoarthritis. Arthritis Rheum 41: 1266-74, 1998

18) Aigner T, Kim HA: Apoptosis and cellular vitality issues in osteoarthritic cartilage degeneration. Arthritis Rheum 46(8): 1986-96, 2002

19) Kim HA, Lee YJ, Seong SC et al: Apoptotic chondrocyte death in human osteoarthritis. J Rheumatol 27(2): 455-62, 2000

20) Kim SJ, Hwang SG, Shin DY et al: p38 kinase regulates nitric oxide-induced apoptosis of articular chondrocytes by accumulating p53 via NF-kappaB-dependent transcription and stabilization by serine 15 phosphorylation. J Biol Chem 6: 277(36): 33501-8, 2002

21) Nishida K, Doi T, Inoue H: The role of nitirc oxide in arthritic joint- a therapeutic target? Review. Modern Rheumatol 10: 63-67, 2000

22) Taskiran D, Stefanovic-Racic M, Georgescu H et al: Nitric oxide mediates suppression of cartilage proteoglycan synthesis by interleukin-1. Biochem Biophys Res Commun 200: 142-8, 1994

23) Pelletier JP, Lascau-Coman V, Jovanovic D et al: Selective inhibition of inducible nitric oxide synthase in experimental osteoarthritis is associated with reduction in tissue levels of catabolic factors. J Rheumatol 26: 2002-14, 1999

24) Pelletier JP, Jovanovic DV, Lascau-Coman V et al: Selective inhibition of inducible nitric oxide synthase reduces progression of experimental osteoarthritis in vivo. Possible link with the reduction in chondrocyte apoptosis and caspase 3 level. Arthritis Rheum 43: 1290-9, 2000

25) Mathy-Hartert M, Deby-Dupont GP, Reginster JY et al: Regulation by reactive oxygen species of interleukin-1 beta, nitric oxide and prostaglandin E_2 production by human chondrocytes. Osteoarthritis Cartilage 10(7): 547-55, 2002

26) McCartney-Francis N, Allen JB, Mizel DE et al:

Suppression of arthritis by an inhibitor of nitric oxide synthase. J Exp Med 1 178(2): 749-54, 1993

27) Connor JR, Manning PT, Settle SL et al: Suppression of adjivant-induced arthritis by selective inhibition of inducible nitric oxide synthase. Eur J Pharmacol 273: 15-24, 1995

28) Kato H, Nishida K, Inoue H: Effect of NOS2 gene deficiency on the development of autoantibody mediated arthritis and subsequent articular cartilage degeneration. J Rheumatol 30: 247-55, 2003

29) Badger AM, Roshak AK, Cook MN et al: Differential effects of SB 242235, a selective p38 mitogen-activated protein kinase inhibitor, on IL-1 treated bovine and human cartilage/chondrocyte cultures. Osteoarthritis Cartilage 8(6):434-43, 2000

30) Goodstone NJ, Hardingham TE: Tumour necrosis factor alpha stimulates nitric oxide production more potently than interleukin-1beta in porcine articular chondrocytes. Rheumatology(Oxford)41(8): 883-91, 2002

31) Relic B, Bentires-Alj M, Ribbens C et al: TNF-alpha protects human primary articular chondrocytes from nitric oxide-induced apoptosis via nuclear factor-kappaB. Lab Invest 82(12): 1661-72, 2002

32) Vuolteenaho K, Moilanen T, Hamalainen M et al: Effects of TNFalpha-antagonists on nitric oxide production in human cartilage. Osteoarthritis Cartilage 10(4): 327-32, 2002

33) Wang Y, Lou S: Direct protective effect of interleukin-10 on articular chondrocytes *in vitro*. Chin Med J (Engl) 114(7): 723-5, 2001

34) Leo AB, Lubberts E, Durez P et al: Role of interleukin-4 and interleukin-10 in murine collagen-induced arthritis. Protective effect of interleukin-4 and interleukin-10 treatment on cartilage destruction. Arthritis Rheum 40: 249-60, 1997

35) Kawahito Y, Kondo M, Tsubouchi Y et al: 15-deoxy-$\Delta^{12,14}$-PGJ$_2$ induces synoviocyte apoptosis and suppresses adjuvant-induced arthritis in rats. J Clin Invest 106: 189-97, 2000

36) Bordji K, Grillasca JP, Gouze JN et al: Evidence for the presence of peroxisome proliferator-activated receptor (PPAR) α and γ and retinoid Z receptor in cartilage. PPARγ activation modulates the effects of interleukin-1β on rat chondrocytes. J Biol Chem 275: 12243-50, 2000

（西田圭一郎、土井英之、藤原一夫、井上　一）

Arthroscopic Posteromedial Release for Osteoarthritic Knees With Flexion Contracture

Hideshige Moriya, M.D., Takahisa Sasho, M.D., Sakae Sano, M.D., and Yuichi Wada, M.D.

Purpose: To evaluate the clinical outcomes of a new arthroscopic procedure, arthroscopic postero-medial release (PMR), and its potential use as a treatment option for medial-type osteoarthritic (OA) knees. **Type of Study:** Retrospective analysis of clinical outcomes of a case series. **Methods:** Knees with medial-type OA and flexion contracture were treated with PMR. They were classified using the Kellgren and Lawrence (K/L) radiographic grading system and classified using magnetic resonance imaging (MRI) into smooth (S) or irregular (IR) groups, based on the subchondral contour of the medial femoral condyle. Clinical outcome was evaluated using the Japanese Orthopaedic Association knee score (JOA score), verbal rating scale (VRS), and patient satisfaction. **Results:** Fifty-two patients with 58 OA knees were included in the study. The mean age of the patients at the time of surgery was 71.6 years, the average ROM was from 13° to 129°, and the average follow-up period was 3.3 years. Most of the knees were classified as K/L grade III or IV. Overall, the average JOA score improved to 71.6 points from 56.3 points preoperatively. VRS scores decreased in most patients, and 76% of patients were satisfied at their last follow-up. The JOA score of the K/L grade III knees improved to 76.9 from 60.4 points preoperatively and that of the K/L grade IV knees improved to 69.5 from 55.3 points. The improvement in JOA score was less for the IR group, from 54.5 to 66.2 points, than for the S group, from 62.3 to 79.6 points. Five knees from the IR group and 1 from the S group were converted to total knee arthroplasty. **Conclusions:** Knees with relatively advanced OA, for which arthroscopic debridement has conventionally been contraindicated, can be treated with PMR if they are selected properly based on MRI findings. **Level of Evidence:** Level IV, case series. **Key Words:** Arthroscopy—Knee—Osteoarthritis—Debridement—MRI—Contour.

The application of arthroscopic procedures to the osteoarthritic (OA) knee is thought to be limited to the initial stages of the disease. Of the various arthroscopic procedures, arthroscopic debridement is a widely performed surgical procedure and its effectiveness is accepted by many orthopaedic surgeons.[1-5] Some authors recommend that it should be restricted to patients in the early stages of OA,[6] and some recommend that it should be limited to patients younger than 60 years who have minimal deviation of

the mechanical axis.[7,8] However, even when patients are selected properly, the long-term results of this procedure appear to be less than satisfactory because approximately 10% to 50% of patients need total knee arthroplasty (TKA) within several years.[4,9,10] Some even imply that arthroscopic debridement produces only a placebo effect.[11] However, the merits of arthroscopic surgery as a treatment option for OA knees should be considered.

In 2001, Leon et al.[12] reported that their arthroscopic procedure, named arthroscopic decompressive medial release (ADMR), provided excellent results for medial-type osteoarthritis. Their technique is to unload the medial compartment by releasing the medial capsule and medial collateral ligament (MCL) through the portals used for arthroscopy. They cut the medial third of the capsule transversely 1.5 cm proximal to the medial meniscus, and also cut the MCL transversely at the same level. They attribute their success
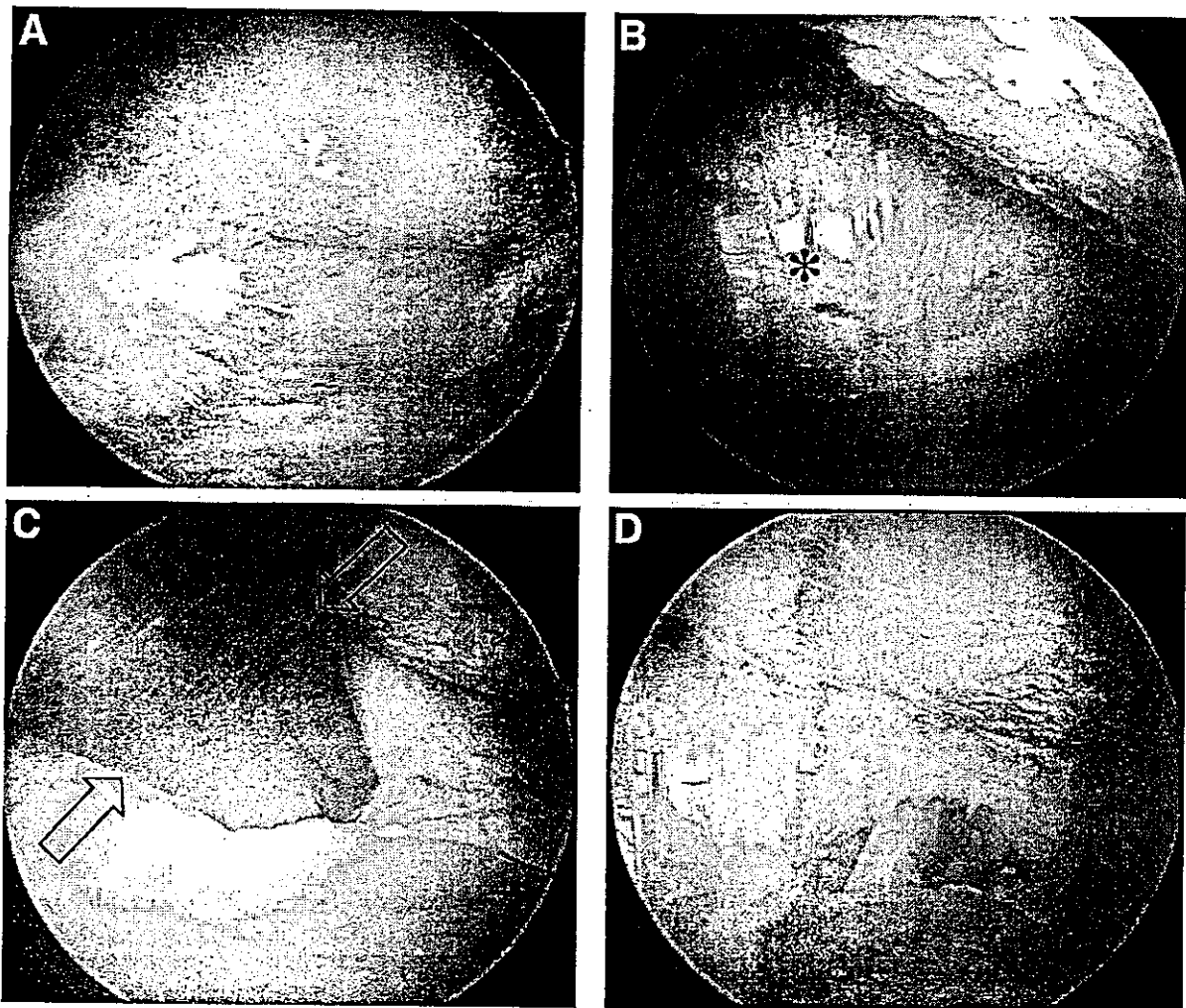
FIGURE 1. The arthroscopic PMR method. (A) Typical arthroscopic findings of the medial compartment in our series are presented. Extended eburnated areas were observed both on the femoral condyle and the tibial plateau. Scanty patches of fibrous tissue were also observed. The medial meniscus was highly degenerated and torn. (B) The first step of PMR is subtotal meniscectomy: the middle-to-posterior segment of the meniscus is excised until the joint capsule (*) is visible. (C) Then the joint capsule, together with the attachment of MCL, is exfoliated from the medial tibial plateau. A periosteal elevator (open arrows) is used for this step. After the meniscectomy and release of the medial side of the joint, valgus and extension stress is applied to the knee joint to widen the joint space of the medial compartment. This will allow the extension of the knee joint as much as possible and will create valgus instability at 30° of flexion. (D) The tendon of the semimembranosus is visible through the opened capsule.

to a decreased adduction moment and increased external rotation. In 1960, Loeffler[13] reported on a procedure including open resection of MCL for releasing the medial side of the knee joint as a treatment for knees with medial-type OA. Several authors reported success with this technique with middle- to long-term follow-up.[14,15] We started to use arthroscopic release of the medial side of the knee joint in 1997, based on the successful results described in these reports as well as on our frequent observation of changes in the

adhesion of the medial joint capsule to the medial tibial plateau when we perform arthroscopic debridement for medial-type OA knee with flexion contracture. In this study, we report the results of our arthroscopic procedure, which we call arthroscopic posteromedial release (PMR). We release the medial compartment of the knee joint by exfoliating the medial capsule and MCL from the medial tibial plateau after meniscectomy. We have applied this procedure to medial-type OA knees with flexion contracture that
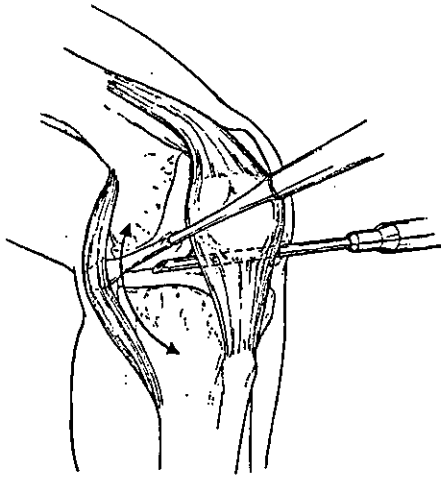
FIGURE 2. Arthroscopic PMR schematic: The medial side of the joint is released with a periosteal elevator under arthroscopy.

would conventionally be considered unsuitable for arthroscopic debridement. We first classified the knees based on magnetic resonance imaging (MRI) criteria and then analyzed the outcomes based on this classification.

METHODS

Fifty-eight medial-type OA knees in 52 patients with flexion contracture were treated with arthroscopic PMR in our hospital. A single surgeon performed all the procedures. Gender, age, radiographic grading using the Kellgren and Lawrence (K/L) system, range of motion (ROM), and the deviation of the

axis on a standing radiograph were recorded at the time of the operation. All the patients had previously been treated conservatively, but because of their persisting knee pain, they had chosen to receive this additional treatment. Our procedure was applied to patients whose symptoms were restricted to the medial side of the knee joint. Patients with asymptomatic patellofemoral joint arthritic involvement were included in this series.

During PMR, we performed arthroscopic debridement, including meniscectomy of the degeneratively torn medial meniscus, excision of the unstable cartilage flap, and release of the joint capsule together with the MCL from the medial tibial plateau (Figs 1 and 2). Our meniscectomies were subtotal, i.e., the posterior two thirds of the medial meniscus was totally removed. Most intra-articular operations can be performed through the conventional two portals, i.e., the lateral and medial infra-patellar portals, but in our experience using midmedial or posteromedial portals made the meniscectomy of the posterior horn of the medial meniscus easier. Following the intra-articular procedure, valgus and extension stress were applied to the knee joint to further the release. Usually we heard a popping sound at this step. If we were unable to obtain enough joint space, i.e., if full extension and valgus instability at 30° of knee flexion were not obtained, we cut the tendon of the semimembranosus muscle. If this was not sufficient, we then cut the MCL transversely at the level of 1 cm below joint line. We did not do any further release if we could not achieve full extension after cutting those 2 structures. We injected hyaluronan intra-articularly once a week for 5 weeks postoperatively. Walking was encouraged from
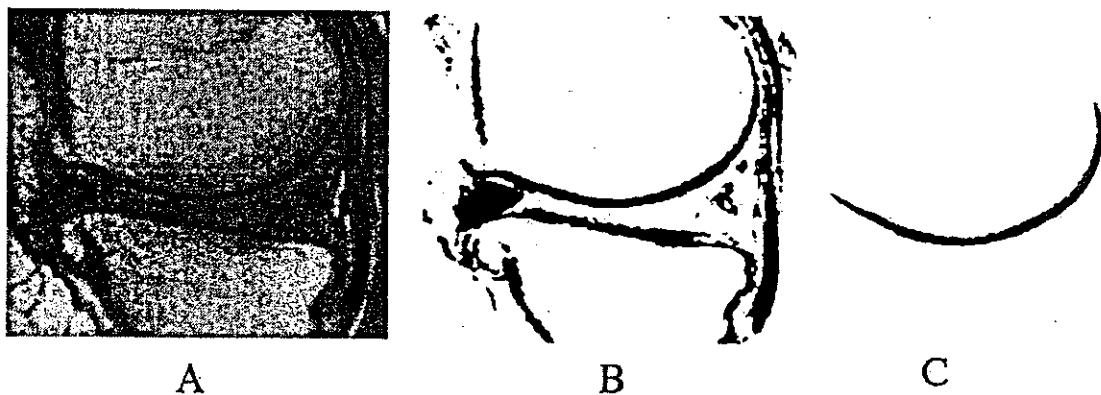

A　　　　　　　　　　B　　　　　　　C

FIGURE 3. Extraction of the contour of the medial femoral condyle. (A) A proton-weighted sagittal image of the center of the medial compartment was scanned and (B) converted into a black and white image using image software. (C) The contour of the medial femoral condyle was extracted from this image and used for further assessment.
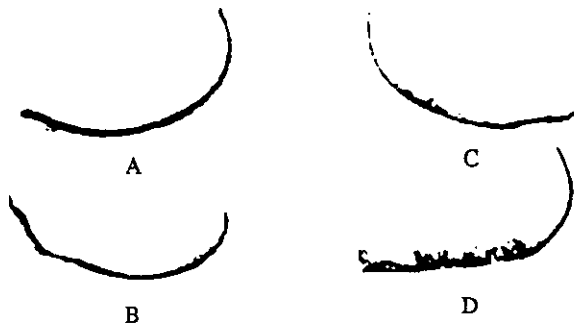
FIGURE 4. Classification of the contour of the medial femoral condyle. (A, B) Contour of the S group: Knees with medial femoral condyles with smooth contours or with minimum irregularity on MRI were classified as the S group. (C, D) Contour of the IR group: Knees with medial femoral condyles with irregular contours were classified as the IR group.

the day following surgery, as tolerated. Patients were evaluated at 3, 6, 12, 18, 24, 36, and 48 months after surgery. Clinical evaluation was performed using the Japanese Orthopaedic Association knee score (JOA score),[16,17] verbal rating score (VRS), and patient satisfaction, which were evaluated at the time of each follow-up. The JOA score is composed of 4 items: (1) pain on walking, (2) pain on ascending or descending stairs, (3) ROM, and (4) joint effusion. The VRS was used to estimate the severity of knee pain at the time of follow-up; patients were asked to rate their pain on a scale from 0 to 10, where the preoperative knee pain corresponded to 10. Patients rated their satisfaction as very satisfied, moderately satisfied, uncertain, or unsatisfied. The clinical outcomes of patients available for more than 2 years of follow-up are presented in this report. All of the evaluations were performed by a single orthopaedic knee surgeon who did not operate on any of the patients.

In addition to the overall analysis, we divided patients into 2 subgroups according to radiographic grade and preoperative MRI findings focusing on the regularity of the contour of the femoral condyle. The clinical outcome of each subgroup was compared using the JOA score. Only patients with knees rated grade III and IV in the K/L system were recruited. All MRI examinations were performed with a Signa 1.5-Tesla imager (GE Medical Systems, Milwaukee, WI), and proton-weighted images were used for evaluating the contour (FSE TR: 2000, TE: 12 msec, ETL: 4, time: 4 min 24 sec). To assess the regularity of the contour of the medial femoral condyle, we used computer image analysis. Sagittal MRIs of the medial femoral condyle were captured into a computer

(PowerMac G3; Apple, Tokyo, Japan) using an image scanner (GT-7600; Epson, Tokyo, Japan), and converted into black and white images (Photoshop 5.0; Adobe, Tokyo, Japan). To determine the threshold between black and white, histograms of the intensity of the dots making the images were used. We determined the threshold so that only the structures with low signal intensity remained while those with iso-intensity to high intensity were deleted (Fig 3). After this manipulation, only the contour of the medial femoral condyle was extracted for evaluation. Patients whose medial femoral condyle was seen as smooth or with minimum irregularity on MRI were classified as the S group (Fig 4A and B), and those depicted with irregular contours on MRI were classified as the IR group (Fig 4C and D). Three knee surgeons independently classified the images as S or IR. If there was discrepancy, the decision was made by the majority.

A histologic examination was performed on specimens removed at the time of TKA. Pieces of bone cut out from the weight-bearing area of the medial femoral condyle were fixed with 10% (vol/vol) formaldehyde for 48 hours and decalcified with 20% EDTA for 10 days. The specimens were then processed and embedded in paraffin. Sections were cut at a thickness of 6 μm on a microtome and stained with H&E.
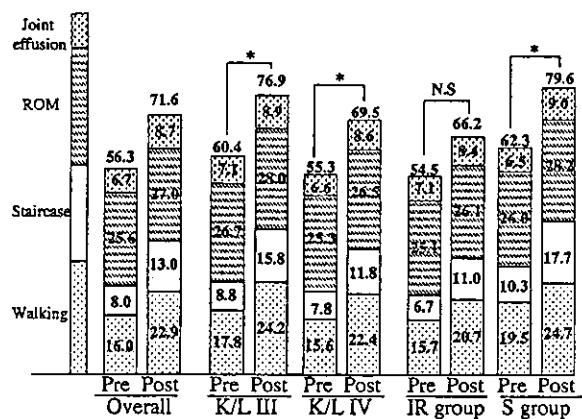

FIGURE 5. Comparison of the JOA scores before and after PMR. Average preoperative and postoperative JOA scores at the time of final follow-up are presented. The overall result is presented in the left 2 columns. Average preoperative and postoperataive JOA scores for subgroups that were classified with radiographic grading (grade III in the K/L grading and grade IV) as well as those divided by MRI findings (the IR group and the S group) are presented for comparison. Statistical analysis for comparing preoperative and postoperative JOA score was performed with the Wilcoxon signed-rank test. $P < .01$ was taken to be statistically significant. The P value for the IR group is more than 0.01 ($P = .011$), indicating a nonsignificant change. *, $P < .01$.
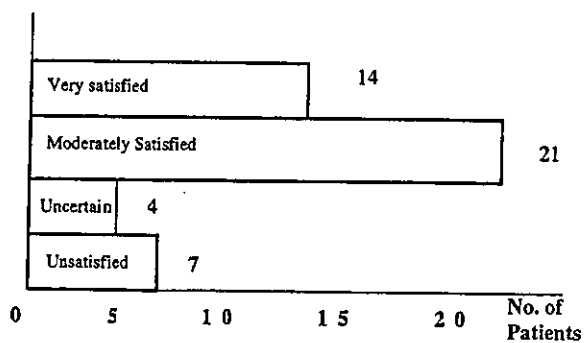
FIGURE 6. The patients' satisfaction at the time of final follow-up is presented. Their level of satisfaction was divided into 4 categories. The number of patients for each category is shown. Each patient who received a bilateral operation is counted as 1 patient on this measure.

Statistical analysis for comparing preoperative and postoperative JOA score was performed using the Wilcoxon signed-rank test. $P < .01$ was considered to be statistically significant.

RESULTS

Fifty-eight medial-type OA knees in 52 patients (37 female and 15 male) with flexion contracture were treated with arthroscopic PMR in our hospital. The
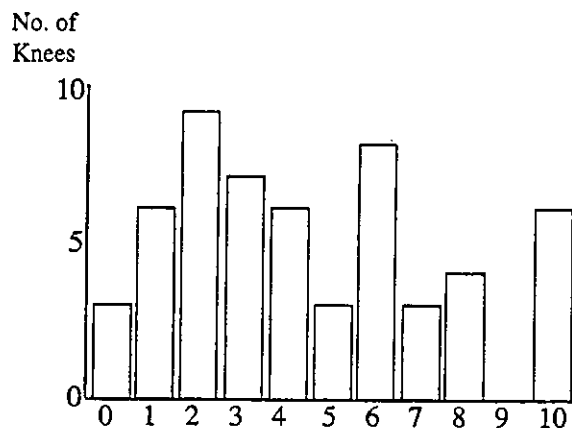

FIGURE 7. A VRS was used to assess the intensity of knee pain. The horizontal axis represents the intensity of the pain and the vertical axis represents the number of knees.

mean age of the patients at the time of surgery was 71.6 years (range, 47 to 84 years). The average ROM was from 13° to 129°. Six patients received bilateral surgeries; 2 were treated with simultaneous operations and 4 were treated with an interval of 10 to 16 months between operations. Seventeen knees were K/L grade III and 40 knees were grade IV. One case was classified as K/L grade II with flexion contracture of 10°.
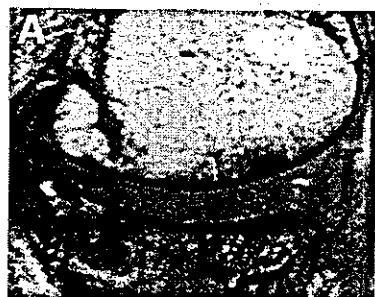

FIGURE 8. Histology of bones with irregular contours: (A) A sagittal MR image of the middle of the medial compartment of the knee joint. (B) Extraction of contour from image A revealed a medial femoral condyle, corresponding to the subchondral bone, with an irregular contour. (C) H&E staining revealed that the irregular contour was produced by the presence of multiple pseudo-cysts (*). Specimens were obtained at the time of TKA.
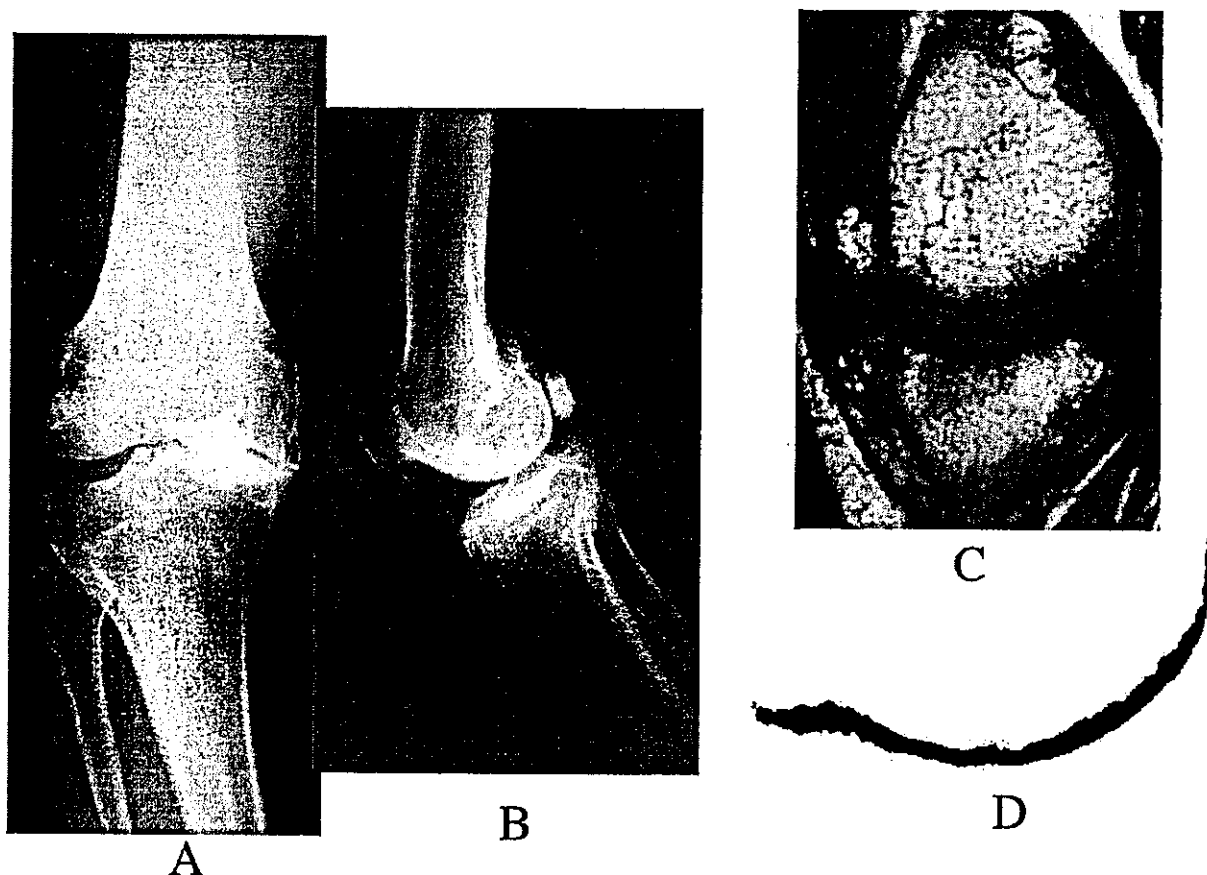
Figure 9. Case 1: A 76-year-old man with varus deformity of 7° was treated with arthroscopic PMR. (A) Standing anteroposterior radiograph showed a highly reduced joint space in his medial compartment. (B) Lateral radiograph showed slight arthritic changes in the patellofemoral (PF) joint. (C, D) MRI showed minimal irregularity in terms of the contour of the medial femoral condyle.

The patients had an average of 2.5° varus knee deformity.

Fifty-two knees belonging to 46 patients were available for more than 2 years of follow-up; the average follow-up period was 3.3 years (range, 2 to 4.8 years). Of these knees, 1 was K/L grade II, 16 were grade III, and 35 were grade IV.

Overall, the average JOA score improved from 56.3 points preoperatively to 71.6 points postoperatively (Fig 5). The average ROM at the time of last follow-up was from 6° to 130°. Seventy-six percent of patients (35 of 46 patients) were satisfied at their last follow-up (Fig 6). The VRS scores were reported as 0 to 2 for about one third of the knees (18 of 52 knees) and were not more than 5 for 65% of the knees (34 of 52 knees) (Fig 7). Although the knees exhibited valgus instability at 30° during follow-up examination,

no patients were apprehensive that the knee would give way on walking.

The average JOA score for the K/L grade III knees improved to 76.9 from 60.4 points preoperatively, and that of the K/L grade IV knees improved to 69.5 from 55.3 points (Fig 5). The improvement in JOA scores was statistically significant for both groups.

Twenty-two knees were classified into the IR group based on MRI, and 24 knees were placed into the S group. MRI examinations of the other 6 knees were either not performed or not judged because of their poor image quality. The JOA score of the IR group improved to 66.2 points from 54.5 points preoperatively and that of the S group improved to 79.6 points from 62.3 points preoperatively (Fig 5). The postoperative JOA score was statistically higher only for the S group. Histologic examina-
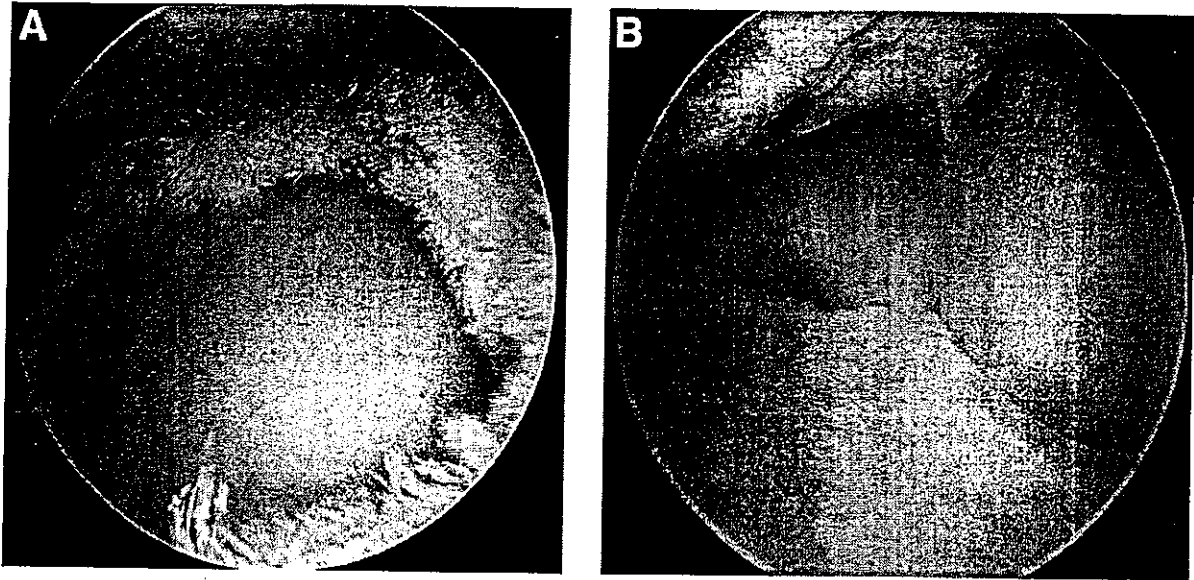
FIGURE 10. Second-look arthroscopy of case 1: (A) The preoperative state of the medial compartment. Extended eburnation of cartilage was observed on both femur and tibia. (B) Neither inflammatory synovium nor re-adhesion of released capsule was found in the medial compartment one year after PMR.

tion revealed that the irregularities of the femoral condyle seen on MRI were the result of microscopic multicystic changes of the subchondral bone (Fig 8).

A total of 6 knees were converted to TKA because of persistent knee pain. Five knees out of the 6 TKA cases belonged to the IR group and only 1 case belonged to the S group. The time from PMR to TKA ranged from 1.3 to 2.5 years.

Case 1

A 76-year-old man with varus deformity of 7° was treated with PMR. His radiograph was stage IV in the K/L system (Fig 9A). His JOA score was 55 preoperatively but improved to 80 points by 6 months after the PMR and was maintained at 80 points for 3 years postoperatively. His MRI showed minimal irregularity in terms of the contour of the medial femoral condyle (Fig 9B). This patient underwent arthroscopy just 1 year after PMR due to locking caused by the free body, which enabled us to see the state of the medial compartment at that time. Figure 10A shows the preoperative state of his medial compartment and Fig 10B shows the state 1 year after PMR. Extended eburnation of the joint surface was observed both on the femur and tibia before PMR (Fig 10A). Neither inflammatory synovitis nor re-adhesion of the released capsule was

found in the medial compartment of his knee joint one year after PMR (Fig 10B).

Case 2

A 59-year-old woman with 1° of varus deformity was treated with PMR. A radiograph showed her knee was K/L grade III. Her MRI was classified as belonging to the IR group (Fig 11). Her JOA improved from 60 points preoperatively to 65 points 1.5 years postoperatively. The patient was not satisfied with the result.

DISCUSSION

In this report we present the clinical results of our arthroscopic PMR procedure as a surgical treatment option for medial-type OA knees. Overall, the JOA score improved 15 points, to an average score of 71.6 points following PMR. This is not as good as the results of TKA; in our hospital, 80 OA knees treated with TKA achieved an average score of 80.0 with an average follow-up of 2.5 years.[18] However, considering that all the knees in this series had flexion contracture and their radiographic grading showed advanced OA changes, this procedure is certainly of potential benefit for some patients because this arthroscopic operation is performed with the use of only 2 to 3 arthroscopic portals and does not lead to loss of
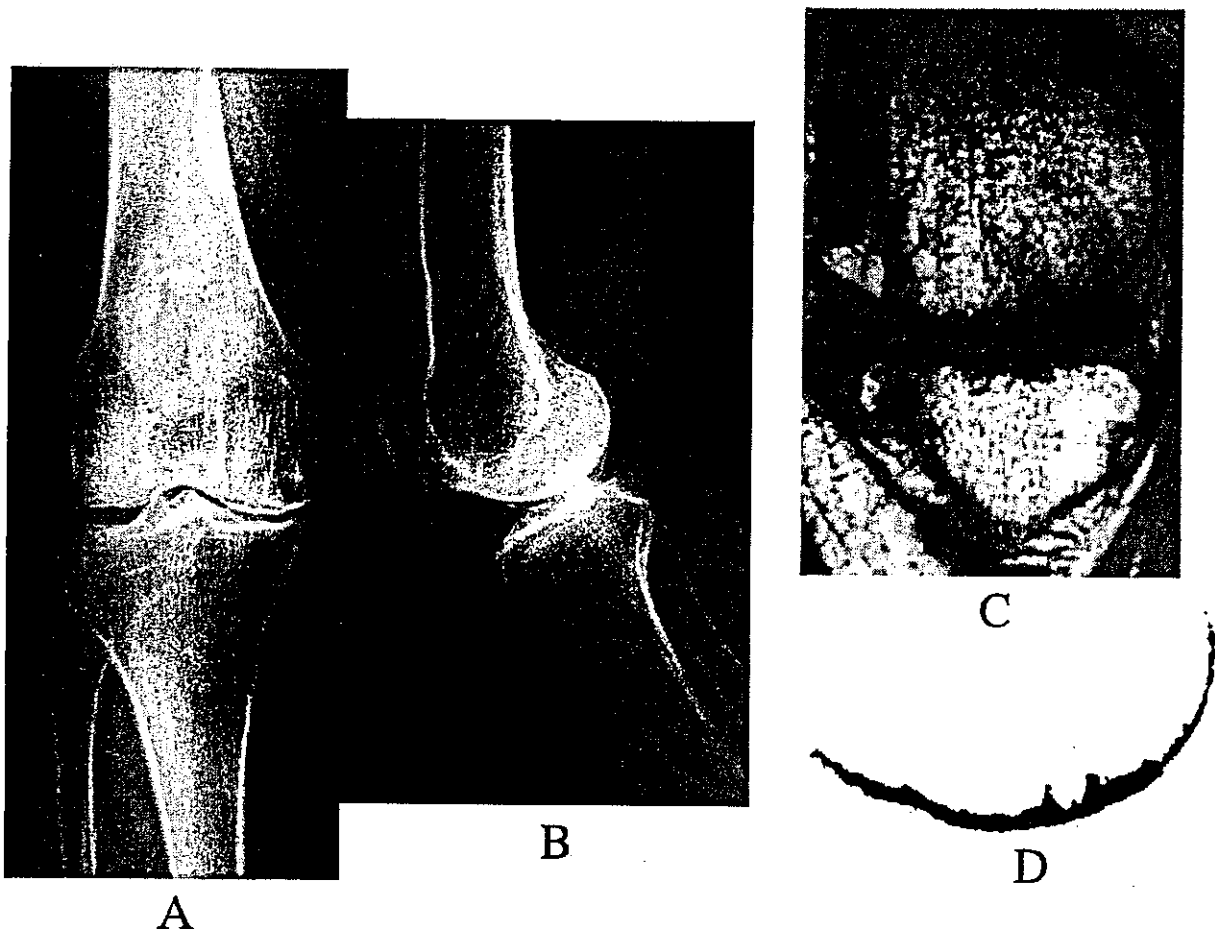
Figure 11. Case 2: A 59-year-old woman with 1° of varus deformity was treated with PMR. (A) Her radiograph indicated osteoarthritis of grade III in the K/L system. (B) Minimal arthritic change was observed in the patellofemoral joint. (C, D) Sagittal MRI of her medial compartment was used to classify her knee into the IR group.

ROM. The knees of the S group showed greater improvement, from 62.3 points preoperatively to 79.6 points postoperatively, a result equivalent to that of the TKA cases. We focused on the contour of the medial femoral condyle on MRI because our earlier study revealed that irregularity of the contour of the medial femoral condyle serves as an indicator of the clinical severity of medial-type OA.[19] In the present study, the patients' ages were somewhat different between the S and the IR group, although the radiographic grading of the 2 groups was almost identical (Table 1). Thus, the MRI findings are a significant factor in determining the clinical outcome of PMR. In contrast, grade IV knees obtained a statistically significant improvement in the JOA score, as did those of

TABLE 1. *Background of Patients*

	S Group	IR Group
Age (yr)	68.6 (47-82)	73.7 (58-90)
Lateral femorotibial angle	181.8° (177°-185°)	182.5° (177°-190°)
K/L Radiographic grade		
I	0	0
II	1	0
III	6	5
IV	12	13

NOTE. Basic information about the patients involved in the S or the IR classification is presented. Average age at the time of operation, varus deformity evaluated by standing anteroposterior radiograph, and distribution of Kellgren & Lawrence radiographic gradings are described.
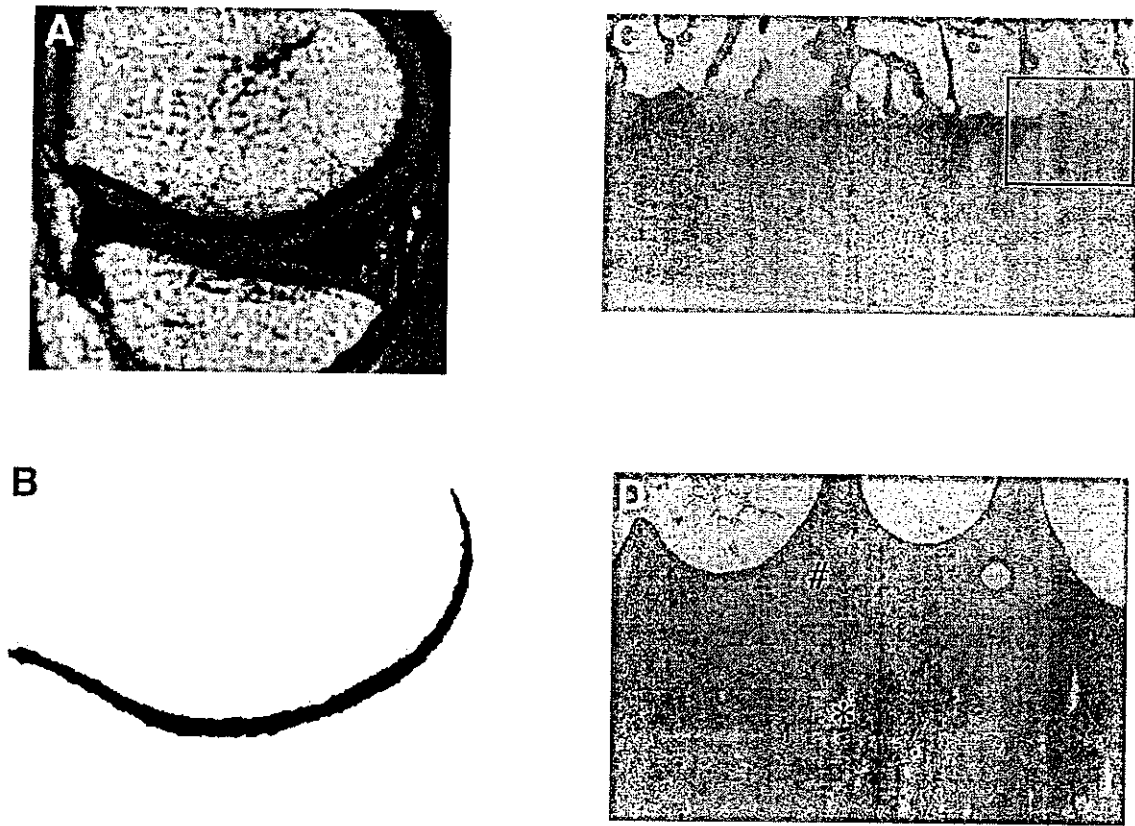
Figure 12. Histologic examination of a knee with a medial femoral condyle of smooth contour on MRI. (A) The original MRI and (B) an extracted contour. (C, low magnification; D, high magnification) Histologic examination of medial femoral condyle from this specimen shows the intact cartilage and regularly corrugated subchondral bone plate (#, subchondral bone; *, cartilage). The open box in C represents the area presented in D.

grade III, implying that radiographic grading does not decisively predict the outcome of PMR.

Based on pathologic examination, we concluded that the knees placed in the IR group contained advanced OA because the subchondral bone described on MRI as irregularly contoured was filled with multiple pseudocysts (Fig 8). In contrast, the smooth contours showed a regular subchondral pattern and no cysts (Fig 12; this specimen was obtained from a patient who suffered from a patellofemoral type OA knee and received TKA and who is not a case in this series). We conjecture that this pathologic change could lessen the effectiveness of bone-preserving procedures such as arthroscopic surgery or osteotomy. Several authors have reported benefits from arthroscopic debridement only when it was applied to knees in the early stages of OA.[6,7,8,20] In general, once OA knees have advanced beyond a certain stage, no arthroscopic treatment appears to be effective.

In 2001, Leon et al.[12] reported the clinical results of their ADMR procedure. Although they did not use any rating system for the assessment, they reported that their technique produced good results in 100% of their cases, and advocated the merit of releasing the medial side of the knee joint for medial-type arthritic knees. They stated that knees with more than grade III in the Ahlbach grading system are suitable for ADMR, which means that the OA of their patients was as severe as ours in terms of radiographic grading.[21] ADMR and PMR are different in the level of release and the approach to the medial meniscus. In ADMR, the release of the capsule is performed proximal to the medial meniscus but in PMR it is performed at the level of the tibial attachment. In ADMR, medial menisci are treated only when they are torn, but in PMR, medial menisci are excised in all cases; we observed that all of our cases had degeneratively torn menisci. ADMR and PMR are the same in terms of releasing

the medial side of the knee joint, but the clinical results of ADMR seemed to be better than our series. This may be simply due to the different techniques, but it is also possible to attribute this discrepancy to patient selection, the assessment method, or differences in lifestyle. However, the patient information that Leon et al. presented in their report was too restricted to allow comparison of these factors here.[12] We can state that we observed degeneratively torn menisci in all our cases without exception, which is consistent with the report by Jackson and Dieterichs[6] that degenerative menisci were seen in all of their patients with eburnated knees. On the other hand, some of the cases of Leon et al. had intact menisci, which may indicate that they treated some patients with earlier stages of OA in their series. We can also state that when TKA is required in the future, PMR gives the advantage of retaining the MCL as a ligamentous structure.

For postoperative care, we used hyaluronan once a week for 5 weeks with the expectation of inhibiting the released tissue from re-adhering to the medial tibial plateau. Hyaluronan is known to inhibit adhesive reactions from occurring in operatively damaged tissue.[22-24]

In conclusion, knees with relatively advanced medial-type OA with flexion contracture can potentially be successfully treated with PMR if their medial compartment is classified as S using MRI.

REFERENCES

1. Livesley PJ, Doherty M, Needoff M, Moulton A. Arthroscopic lavage of osteoarthritic knees. *J Bone Joint Surg Br* 1991;73: 922-926.
2. Hubbard MJS. Articular debridement versus washout for degeneration of the medial femoral condyle. *J Bone J Surg Br* 1996;78:217-219.
3. Shannon FJ, Devitt AT, Poyton AR, Fitzpatric P, Walsh MG. Short-term benefit of arthroscopic washout in degenerative arthritis of the knee. *Int Orthop* 2001;25:242-245.
4. McGinley BJ, Cushner FD, Scott WN. Debridement arthroscopy: 10-year follow-up. *Clin Orthop* 1999;367:190-194.
5. Richards RN Jr, Lonergan RP. Arthroscopic surgery for relief of pain in the osteoarthritic knee. *Orthopedics* 1984;7:1705-1707.
6. Jackson RW, Dieterichs C. The results of arthroscopic lavage and debridement of osteoarthritic knees based on the severity of degeneration: A 4- to 6-year symptomatic follow-up. *Arthroscopy* 2003;19:13-20.
7. Salisbuy RB, Nottage WM, Gardner V. The effects of alignment on results in arthroscopic debridement of the degenerative knee. *Clin Orthop* 1985;198:268-272.
8. Harwin SF. Arthroscopic debridement for osteoarthritis of the knee: Predictor of patient satisfaction. *Arthroscopy* 1999;15: 142-146.
9. Bert JM, Maschka K. The arthroscopic treatment of unicompartmental gonarthrosis: A five-year follow-up study of abrasion arthroplasty plus arthroscopic debridement and arthroscopic debridement alone. *Arthroscopy* 1989;5:25-32.
10. Rand JA. Role of arthroscopy in osteoarthritis of the knee. *Arthroscopy* 1991;7:358-363.
11. Moseley JB, O'Malley K, Petersen NJ, et al. A controlled trial of arthroscopic surgery for osteoarthritis of the knee. *N Engl J Med* 2002;347:81-88.
12. Leon HO, Blanco CER, Guithrie TB. Arthroscopic decompressive medial release of the varus arthritic knee: Expanding the functional envelope. *Arthroscopy* 2001;17:523-526.
13. Loeffler F. Die operative Behandlung der schweren schmerzhaften Arthrose des Kniegelenkes. *Zentralbl Chir* 1960;85: 1020-1023.
14. Schonbauer HR. Experience and results with the Loeffler operation for osteoarthritis of the knee joint. *Arch Orthop Unfallchir* 1976;85:337-346.
15. Reichel F; Muller-Stephann H. Loeffler's capsulotomy in advanced varus gonarthrosis. *Beitr Orthop Traumatol* 1988;35: 453-457.
16. The Japanese Orthopaedic Association Japanese Knee Society. *Assessment criteria for knee diseases and treatments.* Tokyo: Kanehara, 1994.
17. Wakabayashi S, Akizuki S, Takizawa T, Yasukawa Y. A comparison of the healing potential of fibrillated cartilage versus eburnated bone in osteoarthritic knees after high tibial osteotomy: An arthroscopic study with 1-year follow-up. *Arthroscopy* 2002;18:272-278.
18. Song L, Suzuki M, Tsuneizumi Y, Tsukeoka T, Moriya H. Clinical results of Hi-tech knee II total knee arthroplasty [in Japanese]. *Hiza* 2003;24:180-182.
19. Sasho T, Wada Y, Nakagawa K, Fujita K, Takahashi K, Moriya H. MRI as an indicator of disease progression and severity of osteoarthritis of the knee [in Japanese]. *Hiza* 2001; 22:222-225.
20. Fond J, Rodin D, Ahmad S, Nirschl RP. Arthroscopic debridement for the treatment of osteoarthritis of the knee: 2- and 5-year results. *Arthroscopy* 2002;18:829-834.
21. Petersson IF, Boegard T, Saxne T, Silman AJ, Svensson B. Radiographic osteoarthritis of the knee classified by the Ahlback and Kellgren & Lawrence systems for the tibiofemoral joint in people aged 35-54 years with chronic knee pain. *Ann Rheum Dis* 1997;56:493-496.
22. Abitbol JJ, Lincoln TL, Lind BI, Amiel D, Akeson WH, Garfin SR. Preventing postlaminectomy adhesion. A new experimental model. *Spine* 1994;19:1809-1814.
23. Burns JW, Skinner K, Colt J, et al. Prevention of tissue injury and post surgical adhesions by precoating tissues with hyaluronic acid solutions. *J Surg Res* 1995;59:644-652.
24. Moro-oka T, Miura H, Mawatari T, et al. Mixture of hyaluronic acid and phospholipid prevents adhesion formation on the injured flexor tendon in rabbits. *J Orthop Res* 2000;18: 835-840.

Distinct roles of Smad pathways and p38 pathways in cartilage-specific gene expression in synovial fibroblasts

Hiroaki Seto,[1,2] Satoshi Kamekura,[1] Toshiki Miura,[1] Aiichiro Yamamoto,[1] Hirotaka Chikuda,[1] Toru Ogata,[1] Hisatada Hiraoka,[1] Hiromi Oda,[1] Kozo Nakamura,[1] Hisashi Kurosawa,[2] Ung-il Chug,[3] Hiroshi Kawaguchi,[1] and Sakae Tanaka[1]

[1]Department of Orthopaedic Surgery, Faculty of Medicine, The University of Tokyo, Tokyo, Japan. [2]Department of Orthopaedics, Juntendo University School of Medicine, Tokyo, Japan. [3]Division of Tissue Engineering, University of Tokyo Hospital, Tokyo, Japan.

The role of TGF-β/bone morphogenetic protein signaling in the chondrogenic differentiation of human synovial fibroblasts (SFs) was examined with the adenovirus vector–mediated gene transduction system. Expression of constitutively active activin receptor–like kinase 3 (ALK3[CA]) induced chondrocyte-specific gene expression in SFs cultured in pellets or in SF pellets transplanted into nude mice, in which both the Smad and p38 pathways are essential. To analyze downstream cascades of ALK3 signaling, we utilized adenovirus vectors carrying either Smad1 to stimulate Smad pathways or constitutively active MKK6 (MKK6[CA]) to activate p38 pathways. Smad1 expression had a synergistic effect on ALK3[CA], while activation of p38 MAP kinase pathways alone by transduction of MKK6[CA] accelerated terminal chondrocytic differentiation, leading to type X collagen expression and enhanced mineralization. Overexpression of Smad1 prevented MKK6[CA]-induced type X collagen expression and maintained type II collagen expression. In a mouse model of osteoarthritis, activated p38 expression as well as type X collagen staining was detected in osteochondrophytes and marginal synovial cells. These results suggest that SFs can be differentiated into chondrocytes via ALK3 activation and that stimulating Smad pathways and controlling p38 activation at the proper level can be a good therapeutic strategy for maintaining the healthy joint homeostasis and treating degenerative joint disorders.

Introduction

Injury to the articular cartilage occurs under various pathological conditions such as trauma, inflammation, and aging (1), and cartilage injury is followed by osteoarthritic changes of the affected joints. Osteoarthritis is the most common degenerative joint disorder, affecting nearly half of the elderly population. Osteoarthritis is characterized by degradation of articular cartilage and overgrowth of cartilage and bone, known as osteophytes, at the periphery of the articular surface, which results in pain and loss of joint function (1, 2). Microscopically, loss of proteoglycan and fibrillation of the articular surface are observed at the early stage of arthritis. At later stages, clefts are formed, and at the end stage, erosive changes in the articular cartilage appear. The high prevalence of this disease results in high costs for treating patients, and therefore the development of good therapeutics for osteoarthritis is a matter of great urgency. Because of the limited capacity of spontaneous healing, the regeneration of intact articular cartilage is one of the most challenging issues in the orthopedic field (3, 4). Transplantation of autologous chondrocytes or mesenchymal progenitor cells and autogenous osteochondral transplantation (mosaicplasty) have been successfully utilized for the repair of focal osteochondral defects (3, 5–11). However, the application of these

technologies is limited to small defects due to the difficulty of obtaining a sufficient amount of cells or tissues.

Synovium is a thin tissue lining the nonarticular surfaces of diarthrodial joints (12). Synovial tissues contain various types of cells, including type A cells, macrophage lineage cells, and type B cells, which are specialized synovial fibroblasts (SFs). It is now widely recognized that synovial tissues are involved primarily in the pathogenesis of arthritic joint disorders such as rheumatoid arthritis by producing the matrix-degenerating enzymes cystein proteases and matrix metalloproteinases (MMPs) and the proinflammatory cytokines interleukin-1 (IL-1) and tumor necrosis factor-α (TNF-α) (12). We previously reported that SFs express a high level of receptor activator of NF-κB ligand, the osteoclast differentiation factor belonging to the TNF-α superfamily (13). In contrast to such catabolic actions, there is accumulating evidence that synovial cells have anabolic effects, leading to bone and cartilage production. Hunziker and Rosenburg reported that synovial cells can migrate into partial-thickness articular cartilage defects, where they proliferate and subsequently deposit a scar-like tissue (14). Nishimura et al. (15) demonstrated SFs show chondrogenic differentiation after being cultured in the presence of TGF-β, and de Bari et al. recently demonstrated that multipotent mesenchymal stem cells could be isolated from human synovial tissues, which differentiated into chondrocytes as well as osteoblasts, adipocytes, and myotubes under proper culture conditions (16, 17). Another dramatic clinical manifestation of the chondrogenic potential of synovial tissues is synovial chondromatosis, a tumor-like disorder characterized by the formation of multiple cartilaginous nodules, which is believed to be benign reactive metaplasia of synovial cells (18). These observations

lead us to speculate that synovial tissues contain multipotent cells with chondrogenic potential that might be involved in the repair process of articular cartilage defects and therefore might provide a good source for engineering articular cartilage.

There is accumulating evidence that TGF-β superfamily cytokines play an essential role in bone and cartilage development. Wozney and coworkers (19) reported that bone morphogenetic proteins (BMPs) induce early cartilage formation, and various studies have shown that TGF-β induces chondrocytic differentiation of undifferentiated mesenchymal cells (20–22). In the present study, we analyzed the role of TGF-β/BMP signaling on chondrogenic differentiation of human SFs by using the adenovirus vector-mediated gene transduction system. The introduction of an activated mutant of ALK3 (constitutively active activin receptor-like kinase 3 [ALK3^{CA}]), also known as BMP type IA receptor, induced chondrocyte-specific marker expression in the cells. ALK3 signaling involves two different downstream cascades, the Smad pathway and the p38 MAP kinase pathway. We used a combination of adenoviral gene delivery and chemical inhibition to analyze the role of these two signaling cascades in inducing differentiation of SF cells toward a chondrocyte phenotype and found that both pathways are essential for chondrogenic differentiation. Interestingly, activation of p38 pathways alone induced markers of terminal chondrocyte differentiation, type X collagen expression and mineralization, which was suppressed by Smad1 coexpression. These results suggest that both the Smad and p38 pathways are necessary for chondrogenic differentiation of SFs and that the balance between these two pathways determines the stage of differentiation.

Methods

Chemicals and antibodies. Alpha-modified minimum essential medium (α-MEM) was purchased from Gibco BRL, Life Technologies Inc. (Rockville, Maryland, USA), and fetal bovine serum (FBS), from Sigma-Aldrich (St. Louis, Missouri, USA). Anti-p38 MAPK and anti-phospho-p38 MAPK (Thr180/Tyr182) were obtained from Cell Signaling Inc. (Cummings Center, Beverly, Massachusetts, USA). Anti-Flag was purchased from Sigma-Aldrich, and anti-hemagglutinin (anti-HA) was from Santa Cruz Biotechnology Inc. (Santa Cruz, California, USA). Anti-phospho-Smad1/5/8, which recognizes the phosphorylated form of Smad1, Smad 5, and Smad8, and anti-phospho-Smad2 were from Cell Signaling Inc. Anti-type II collagen was purchased from Oncogen (Boston, Massachusetts, USA) and anti-type X collagen was from LSL Co. (Cosmo Bio, Tokyo, Japan). Other chemicals and reagents used in this study were of analytical grade.

Isolation of SFs from human synovial tissues. Synovial cells were obtained as previously described (13, 23, 24). In brief, with enzymatic digestion, human synovial cells were isolated from synovial tissues of the knee joints of ten rheumatoid arthritis patients (37–75 years of age; mean, 60.3 years of age) at the time of total knee arthroplasty operations. Written informed consent for subsequent experiments was obtained from each patient. Cells were suspended in α-MEM containing 10% FBS and were cultured in monolayers. After three to five passages, subcultured cells were composed of morphologically uniform fibroblastic cells (SFs) that were free of macrophages. They were infected with adenovirus vectors and cultured in pellets ("pellet culture"). Primary chondrocytes were obtained from articular cartilage resected during the surgeries. Cartilage was minced finely in phosphate-buffered saline (PBS), and chondrocytes were isolated by sequential digestion at 37°C with

0.25% (weight/volume) trypsin for 30 minutes and with 2 mg/ml of clostridial collagenase in α-MEM containing 10% FBS and antibiotics (penicillin at 100 μg/ml and streptomycin at 100 μg/ml) overnight on an orbital shaker. Cells were isolated by centrifugation and were resuspended in α-MEM with 10% FBS. Cells were cultured in monolayers for 1 day and then subjected to RNA isolation.

Constructs and gene transduction. The recombinant adenovirus vectors carrying various molecules that modulate TGF-β superfamily signaling pathways, that is, HA-tagged constitutively active TGF-β/BMP type I receptors (ALK3^{CA}, ALK5^{CA}, and ALK6^{CA}), constitutively active MKK6 (MKK6^{CA}), Flag-tagged Smad1 and Smad6 with CAG [cytomegalovirus IE enhancer + chicken β-actin promoter + rabbit β-globin poly(A) signal] promoter, were generated by the DNA-terminal protein complex method (25–27). SFs were infected with adenovirus vectors following a method previously described (13). In short, subconfluent SFs were incubated with a small amount of medium (α-MEM without serum) that contained the recombinant adenoviruses for 2 hours at 37°C at the indicated multiplicity of infection (MOI) and then with 10 times more medium to which 10% FBS had been added. Infected cells were cultured for additional 3 days for assessment of chondrogenic gene expression or were subjected to pellet culture 24 hours after the infection for histological examination.

Pellet cultures of isolated SFs. After 24 hours of viral infection, adherent cells were trypsinized and cells numbers were ascertained. Aliquots of 5 × 10^5 cells were spun down at 500 g in 15-ml polypropylene conical tubes in 5 ml of α-MEM with ascorbate 2-phosphate (0.1 mM) and 10% FBS. The cells were incubated at 37°C in 5% CO$_2$. Within 24 hours after incubation, the cells formed a single, free-floating pellet. The medium was changed every 2–3 days, and duplicate pellets were harvested after 3 and 7 days for real-time-PCR and Northern blotting and after 3 and 5 weeks for histological and immunohistochemical analysis. For visualization of the chondrogenic differentiation in vivo pellets were transplanted subcutaneously into nu/nu BALB mice (nude mice) after 3 days of pellet culture. Mice were sacrificed 5 weeks after transplantation and the pellets were recovered and subjected to toluidine blue staining as well as immunostaining with anti-type II collagen.

Immunoblotting. All the extraction procedures were performed at 4°C or on ice. Cells were washed with PBS and then lysed by the addition of TNE buffer (1% NP-40, 10 mM Tris-HCl, pH 7.8, 150 mM NaCl, 1 mM EDTA, 2 mM Na$_3$VO$_4$, 10 mM NaF, and 10 μg/ml aprotinin). Lysates were prepared by centrifugation at 10,000 g for 20 minutes. An equal amount (15 μg) of proteins was separated by electrophoresis on 10% SDS-polyacrylamide gels. After electrophoresis, proteins were electronically transferred onto a nitrocellulose membrane. Immunoblotting with specific antibodies was performed with ECL Western blotting reagents (Amersham Co., Arlington Heights, Illinois, USA) according to the conditions recommended by the supplier.

Histology and immunostaining. Pellet cultures were fixed with 3.7% formaldehyde, embedded in paraffin, and cut into sections 4 μm in thickness. Representative sections were subjected to Alcian blue staining, Alizarin red staining, and immunohistochemistry. Alcian blue staining was performed according to the protocol described previously (28). Briefly, after deparaffinization, sections were stained with 0.5% Alcian blue 8GX (Wako, Osaka, Japan) in 0.1 N HCl for 1 hour. Mineralization was assessed by Alizarin red staining. In brief, sections were immersed in Alizarin red solution (40 mM, at pH 4.0) for 8 minutes at room temperature, and nonspecific staining was removed by several washes in distilled water. For immunostaining with anti-type

II collagen or anti–type X collagen, we utilized a CSA Kit (DAKO, Carpinteria, California, USA) following the manufacturer's protocol.

Total RNA extraction and real-time PCR. Total RNA was isolated from SFs with ISOGEN (Wako) following the supplier's protocol. Complementary DNA (cDNA) was synthesized from 1 μg of total RNA with the Superscript II reverse transcriptase kit (Invitrogen, Carlsbad, California, USA). For real-time PCR, the ABI Prism Sequence Detection System 7000 was used. Primers were designed based on sequences obtained from GenBank and amplicons of 50–250 base pairs with a melting temperature of between 55°C and 60°C were selected. Aliquots of first-strand cDNA (1 μg) were amplified with the QuantiTect SYBER Green PCR Kit (Qiagen, Valencia, California, USA) under the following conditions: initial denaturation for 10 minutes at 94°C followed by 40 cycles consisting of 15 seconds at 94°C and 1 minute at 60°C. Data analysis consisted of fold induction, and the expression ratio was calculated from the differences in threshold cycles at which an increase in reporter fluorescence above a baseline signal could first be detected among three samples and was averaged for duplicate experiments. The primers we utilized in real-time PCR to detect sox9, type II collagen, type X collagen, osteocalcin, osteopontin, and GAPDH were as follows: sox9, 5'-AGAAG-GACCACCCGGATTAC-3' and 5'-AAGTCGATAGGGGGCTGTCT-3'; type II collagen, 5'-GGTGGCTTCCATTTCAGCTA-3' and 5'-TACCGGTATGTTTCGTGCAG-3'; type X collagen, 5'-AGGAAT-GCCTGTGTCTGCTT-3' and 5'-ACAGGCCTACCCAAACATGA-3'; osteocalcin, 5'-GTGCAGAGTCCAGCAAAGGT-3' and 5'-CGATAG-GCCTCCTGAAAGC-3'; osteopontin, 5'-ACAGCCAGGACTC-CATTGAC-3' and 5'-ACACTATCACCTCGGCCATC-3'; and GAPDH, 5'-GAAGGTGAAGGTCGGAGTCA-3' and 5'-GAAGATG-GTGATGGGATTTC-3'.

Northern blotting. Equal amounts (15 μg) of RNA were denatured in formaldehyde, separated by 1% agarose gel electrophoresis and transferred to a nitrocellulose membrane (Hybond N⁺) (Amersham Pharmacia, Piscataway, New Jersey, USA), followed by ultraviolet cross-linking. ULTRAHyb hybridization solution (Ambion, Austin, Texas, USA) was used according to the manufacturer's protocol. The blots were hybridized with a cDNA probe labeled with [α-32P]dCTP using Ready-To-Go DNA Labeling Beads (Amersham Pharmacia). Rabbit type II collagen and aggrecan probes were generously provided by Yoshiyasu Iwamoto (Thomas Jefferson University, Philadelphia, Pennsylvania, USA). Membranes were washed in 2× SSC for 15 minutes at 42°C and then in 0.1× SSC for 30 minutes at 65°C. For visualization, X-ray film was exposed to membranes overnight at –80°C.

Osteoarthritis model mice. Osteoarthritic changes were developed in the knee joint by transection of the anterior cruciate ligament (ACL) and medial meniscus (MM) in C57BL/6 mice (mean age, 8 weeks) (29, 30). Briefly, after mice were anesthetized with ketamine and xylazine, a medial parapatellar skin incision was made. The subcutaneous tissues were incised and retracted, along with the articular capsule. The medial compartment of the knee joint was visualized and the ACL and MM were transected with a scalpel, and thereafter the capsule, medial retinaculum, and skin were sutured. Mice were housed in regular individual cages and allowed to exercise. Eight weeks after the surgery, the mice were sacrificed and paraffin-embedded sections of the affected joints were immunostained with anti–type X collagen and anti–phospho-p38 (Cell Signaling Technology Inc).

Results

Adenovirus-mediated gene transduction modulates the Smad and p38 pathways in SFs. We previously reported that adenovirus vectors can effi-

ciently transduce foreign genes into synovial cells both in vitro and in vivo and that adenovirus infection itself does not affect the phenotypes of the cells (13). We constructed adenovirus vectors to analyze the role of ALK signaling as well as the Smad pathways and p38 pathways, which lie downstream of ALK signaling. SFs were infected with adenovirus vectors carrying various signaling molecules that modulate TGF-β superfamily signaling pathways, that is, HA-tagged constitutively active ALK3, ALK5, and ALK6 constitutively active MKK6, and Flag-tagged Smad1 and Smad6, as well as a control virus carrying the β-galactosidase gene (LacZ virus), and gene expression was determined by immunoblotting with specific antibodies. As shown in Figure 1, clear induction of the genes encoding ALK3^{CA}, ALK5^{CA} and ALK6^{CA} was observed by immunoblotting with anti-HA (Figure 1A), and Smad1 and 6, by anti-Flag (Figure 1B). ALK3^{CA} or ALK6^{CA} overexpression induced phosphorylation of Smad1, Smad5, and Smad8 in SFs, and ALK5^{CA}-transduced cells showed Smad2 phosphorylation (Figure 1A). MKK6^{CA} virus infection specifically activated p38 pathways in SFs, and the pathways were also activated in ALK3^{CA}-transduced cells as determined by Western blotting with anti–phospho-p38 (Figure 1C). The increased p38 phosphorylation induced by either ALK3^{CA} or MKK6^{CA} overexpression was suppressed by the p38-selective inhibitor SB203580.

Induction of chondrocyte-specific gene expression by ALK3^{CA} transduction in pellet cultures of SFs. To determine the effects of these transduced gene products on chondrocyte-specific gene expression in SFs, we subjected infected cells to pellet culture. After 7 days of culture, clear induction of type II collagen and aggrecan genes was observed in ALK3^{CA}-transduced cultures by both Northern blot analysis (Figure 2A) and real-time PCR (Figure 2, B and C). Expression of these genes was also observed in ALK6^{CA}-transduced cultures, albeit less efficiently, as shown in Figure 2, B and C, by real-time PCR. Contrary to the strong chondrogenic effects of ALK3^{CA} virus, expression
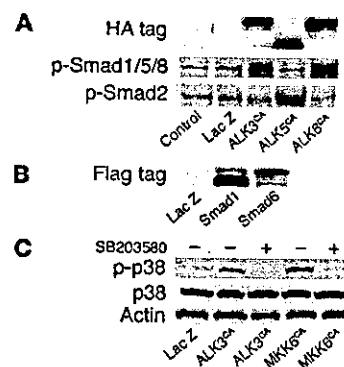
Figure 1
Modulation of intracellular signaling pathways by adenovirus vector–mediated gene transduction into SFs. (A) SFs at passage 3 were transduced with HA-tagged constitutively active ALK3, ALK5, and ALK6, and the expressed products were detected by immunoblotting after 2 days of viral infection. Expression of these genes was detected by immunoblotting with anti-HA and phospho-Smad1, -Smad 5, and Smad8 (p-Smad1/5/8) was observed in cells expressing ALK3^{CA} or ALK6^{CA}, and p-Smad2, in cells expressing ALK5^{CA}. (B) Expression of Smad1 and 6 in SFs was determined by anti-Flag. (C) Adenovirus vector–mediated ALK^{CA} or MKK6^{CA} expression specifically activated p38 pathways in SFs, as determined by Western blotting with anti–phospho-p38 (p-p38). The increased p38 phosphorylation induced by ALK3^{CA} or MKK6^{CA} overexpression was suppressed by the p38-selective inhibitor SB203580.
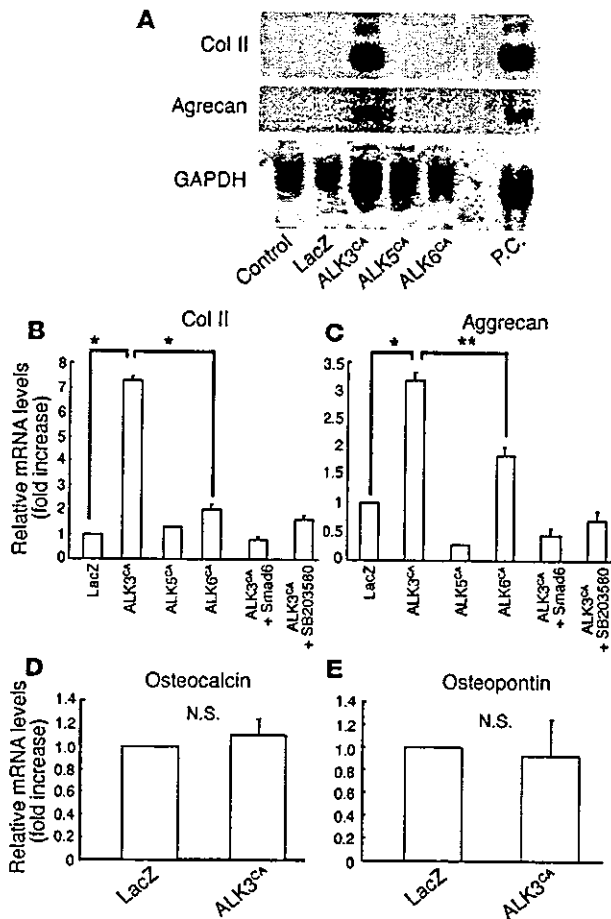
Figure 2
Effects of ALK3^{CA}, ALK5^{CA}, and ALK6^{CA} expression on chondrocyte-specific gene expression in SFs. (A–E) Gene expression in SFs, as determined by Northern blot analysis (A) and real-time PCR analysis (B–E). Subconfluent monolayer SF cultures were infected with adenovirus vectors and they were then subjected to pellet culture 24 hours after viral infection; mRNA extracted from the pellets after 7 days of culture was then analyzed. Expression of type II collagen (Col II) and aggrecan was clearly induced in ALK3^{CA}-expressing cultures, as shown by Northern blot analysis (A) and real-time PCR analysis (B and C); this was suppressed by Smad6 coexpression and SB203580 (B and C). Expression of type II collagen and aggrecan was also observed in ALK6^{CA}-expressing cultures, albeit less efficiently, as shown in B and C by real-time PCR. Neither the osteocalcin nor the osteopontin gene was induced by ALK3^{CA} virus infection (D and E). P.C., positive control, which represents the Northern blotting using mRNA of primary chondrocytes. N.S., not significant; *P < 0.001; **P < 0.005 (significantly different).

of osteocalcin or osteopontin was hardly detectable in the cells (Figure 2, C and D), indicating that hypertrophic and osteogenic differentiation were somehow blocked in these cultures. In contrast, neither type II collagen nor aggrecan gene expression was observed in ALK5^{CA} virus-infected cells (Figure 2, A–C). Type II collagen and aggrecan expression induced by ALK3^{CA} transduction was completely suppressed by coexpression with Smad6 or by SB203580 (Figure 2, B and C).

ALK3 gene transduction increases Alcian blue–positive matrix and type II collagen deposition in pellet cultures of SFs. For histological analysis, cells were subjected to pellet culture 24 hours after the viral infection. After 3 weeks of pellet culture, cells were fixed and examined by Alcian blue staining (Figure 3, A, D, G, and I) and Alizarin red staining and type II collagen immunostaining (Figure 3, B, E, G, and J) and type X collagen immunostaining (Figure 3, C and F). ALK3^{CA} virus-infected cultures showed cartilageous matrix production that was strongly positive for Alcian blue staining (Figure 3D), while no positive staining was observed in LacZ virus-infected cultures (Figure 3A) or ALK5^{CA} virus-infected cultures (Figure 3G), and only weak staining was observed in ALK6^{CA} virus-infected cultures (Figure 3H). No Alizarin red staining was observed in ALK3^{CA}-infected cultures (not shown), indicating that mineralization associated with osteogenic differentiation was not induced. ALK3^{CA} virus-infected SFs showed an oval shape, morphologically reminiscent of chondrocytes (Figure 3D). Immunostaining with

anti-type II collagen showed positive staining in ALK3^{CA} virus-infected pellet cultures (Figure 3E) and weak staining in ALK6^{CA} virus-infected cultures (Figure 3H), while we failed to detect type X collagen in ALK3^{CA} virus-infected cultures (Figure 3F), which suggests an absence of terminal differentiation to hypertrophic chondrocytes. No positive type II collagen immunostaining was detected in LacZ virus-infected cultures (Figure 3B) or ALK5^{CA} virus-infected cultures (Figure 3H).

ALK3^{CA}-transduced SFs after pellet culture form cartilage matrix in vivo. To study chondrogenic differentiation of SFs in vivo, we subcutaneously transplanted the pellets into nude mice. Mice were sacrificed 3 weeks after the transplantation and the pellets were recovered and subjected to histological analysis. The transplanted SF pellets expressing ALK3^{CA} were positively stained for toluidine blue (Figure 4C), which detects proteoglycan components, as does Alcian blue staining. Type II collagen immunostaining was also positive (Figure 4D), indicating the cartilaginous differentiation of the cultures in vivo, while Alizarin red staining was almost undetectable (data not shown). ALK6^{CA} expression also induced chondrogenesis, albeit much less prominently (not shown), while neither LacZ (Figure 4, A and B) or ALK5^{CA} (not shown) expression could induce chondrogenic phenotypes in the cultures. The histological observation was further confirmed by real-time PCR; expression of type II collagen and aggrecan was significantly higher in ALK3^{CA}-transduced pellets (Figure 4, E and F). These results suggest that ALK3^{CA}